Scientific Bases for Establishing Chlorophyll-*a* Thresholds for San Francisco Bay

Martha Sutula[1], Raphael Kudela[2], James D. Hagy III[3], Lawrence W. Harding, Jr.[8], David Senn[9], James E. Cloern[6], Gry Mine Berg[4], Suzanne Bricker[5], Richard Dugdale[7], and Marcus Beck[3]

[1] Southern California Coastal Water Research Project, Costa Mesa, California 92626 USA

[2] Ocean Sciences Department, University of California Santa Cruz, California 95064 USA

[3] U.S. Environmental Protection Agency, Office of Research and Development, Gulf Breeze, Florida 32561 USA

[4] Applied Marine Sciences, Santa Cruz, California USA 95060

[5] NOAA National Centers for Coastal Ocean Science, Silver Spring, Maryland 20910 USA

[6] U.S. Geological Survey, Menlo Park, California 94025 USA

[7] Romberg Tiburon Center, San Francisco State University, Tiburon, California 94920 USA

[8] Department of Atmospheric and Oceanic Sciences, University of California, Los Angeles, California 90095 USA

[9] San Francisco Estuary Institute, Richmond, California 94804 USA

For Submittal to: *Estuarine, Coastal and Shelf Science*

Author for correspondence: Martha Sutula email – marthas@sccwrp.org

Keywords: eutrophication; water quality criteria; dissolved oxygen, HAB, *chl-a*; SPATT

Draft: 03 November 2015

Abstract

San Francisco Bay (SFB) receives high nutrient loads from agricultural runoff, storm water, and treated wastewater effluent from 37 Publically Owned Treatment Works (POTWs), although to date the estuary appears resistant to classic symptoms of eutrophication. Recent trends of increasing chlorophyll-*a* (*chl-a*), harmful algal blooms (HAB), and dissolved oxygen concentrations (DO) suggest this resistance may be weakening. These findings motivated development of water-quality criteria (WQC) for SFB protective from adverse effects of nutrient over-enrichment. WQC consisting of thresholds of phytoplankton biomass as *chl-a* are based on strong relationships between nutrients, *chl-a*, and water-quality impairments in several estuaries. Although plankton ecology is well chronicled for SFB, data from several decades of monitoring have not been used heretofore to support WQC. Here, we analyze long-term data on *chl-a* (1993-2014), phytoplankton species composition (1993-2014), algal toxins (2012-2014), and DO (1993-2014) to derive: (1) quantitative relationships of HAB abundances, toxin levels, and DO to *chl-a;* and (2) *chl-a* thresholds and related uncertainties corresponding to "protected" and "at risk" categories based on WQC for DO and HAB alerts. Although *chl-a* is lower and DO higher in SFB than comparable estuaries experiencing nutrient over-enrichment, we report trends of increasing *chl-a*, declining DO, ubiquitous presence of HAB species, and toxin concentrations exceeding alert levels in ~35% of samples over the last 20 years. Quantile regressions of *chl-a* with HAB abundance and DO were significant, indicating SFB is poised for increased risk of impairments by HAB and low DO with increasing phytoplankton biomass. Coordinated statistical analyses showed *chl-a* thresholds associated with HAB and DO impairments converged on comparable values. We identified monthly mean *chl-a* < 13 mg m^{-3} as an inflection point, below which probabilities for exceeding alert levels for HAB abundances and HAB toxins

were reduced. This HAB-based *chl-a* threshold was similar to a *chl-a* threshold of 13 - 16 mg m^{-3} for meeting the WQC for DO of 7 mg L^{-1}. At the high-end of risk, *chl-a* thresholds from 25 - 40 mg m^{-3} corresponded to a 0.5 probability of exceeding alert levels for HAB abundance, and with consistent excursions of DO in lower South Bay (LSB) and South Bay (SB) below the WQC of 5.0 mg L^{-1} for DO. We suggest that if available nutrients in SFB were assimilated into phytoplankton biomass, mean *chl-a* in all sub-embayments of SFB could reach "high risk" thresholds. These findings justify the establishment of *chl-a* thresholds to support nutrient management of SFB, given uncertainty about the future trajectory of water quality in this important estuarine ecosystem.

Introduction

Nutrient over-enrichment of the world's estuaries has led to multiple ecosystem impairments that express cultural eutrophication (Nixon, 1995; Paerl 1997; Cloern 2001; Diaz and Rosenberg, 2008; Bricker et al. 2008). Identifying specific water-quality goals for nutrients has proven difficult, however, because ecological responses to nutrients are complex. San Francisco Bay (SFB) is a well-documented example of a nutrient-enriched estuary that exhibits this complexity (Cloern and Jassby, 2012). Extensive long-term data suggest that, to date, SFB has been resistant to classic symptoms of nutrient over-enrichment such as high phytoplankton biomass, harmful algal blooms (HAB), and low dissolved oxygen (DO). A number of factors have precluded widespread development of these symptoms in SFB, including high turbidity and concomitant light-limitation of primary productivity, intense tidal mixing that reduces biomass accumulation and DO depletion, and grazing by large populations of filter-feeding clams that regulates phytoplankton biomass in some areas of the bay (cf. Cloern and Jassby, 2012; Cloern et al., 2007; Kimmerer and Thompson, 2014).

Recent evidence suggests resistance to nutrient over-enrichment may be weakening in SFB, such as: (1) a three-fold increase of chlorophyll-*a* (*chl-a*) in South Bay (SB) during summer-fall since 1999 (Cloern et al., 2007); (2) regular occurrences of HAB species (Lehman et al., 2005; Cloern et al., 2005; Cloern and Dufford, 2005); and (3) diurnal depressions of DO to hypoxic conditions with DO < 2.8 mg L^{-1} in restored salt ponds (Thebault et al., 2008; Topping et al., 2009). These observations call for a water-quality framework to inform management actions, consisting of thresholds for key properties that would be "protective" from adverse effects of nutrient over-enrichment. Phytoplankton biomass as *chl-a* is an integrative indicator of nutrient loadings with established links to water-quality impairments, commonly used to assess

eutrophication and support regulatory goals (Bricker et al., 2003; Zaldivar et al., 2008; Harding et al., 2014). Quantitative thresholds leading to management endpoints can be based on deviations from "reference" conditions when data prior to degradation are available (Andersen et al. 2010, 2015), or on ecosystem impairments such as low DO, HAB, or water clarity (e.g., Harding et al., 2014). We lack *chl-a* records for SFB prior to human disturbance, limiting the use of reference conditions, but long-term data on *chl-a* support quantitative analyses of relationships between *chl-a* and potential impairments.

Two pathways of nutrient over-enrichment that culminate in adverse effects on humans, marine mammals, and other aquatic life include: (1) low DO associated with excess organic matter; and (2) increased HAB occurrences (Rosenberg et al., 1991; Diaz and Rosenberg, 1995; Kirkpatrick et al., 2004; Glibert et al., 2005; Baustin and Rabalais, 2009). Recognizing that factors other than nutrients affect low DO and HABs, causal links are established for nutrient loadings, *chl-a*, hypoxia, and HABs (Tett et al., 2007; Heisler et al., 2008; Anderson et al., 2012). Such links have been used to support water quality criteria (WQC) for Chesapeake Bay, relating risk of impairments to increased *chl-a* (e.g., Harding et al., 2014). As in many estuaries, *chl-a* has increased significantly over the past 15-20 years in SFB, amounting to a three-fold increase from the mid-1990s to mid-2000s in South Bay (SB) and Lower South Bay (LSB) (Cloern et al., 2007). Of particular concern are regular occurrences of fall blooms of phytoplankton in SB and LSB since the late 1990s, areas that rarely experienced such outbreaks in the past (Cloern and Jassby, 2012), and significant increases of *chl-a* in other sub-embayments during the same period. Despite these upward trends of *chl-a* and reports of HAB occurrences (see Cloern et al., 1994), routine monitoring for algal toxins has not been conducted (Cloern and Dufford, 2005). Moreover, long-term data on *chl-a*, phytoplankton species composition, and DO

to quantify risk of low DO or HAB occurrences with increasing *chl-a* have yet to be assembled for various sub-embayments of SFB.

Here, we present relationships between DO, HAB, and *chl-a* in SFB to derive quantitative thresholds based on water-quality impairments. We then apply these thresholds as endpoints to support assessments of status and trends of water quality required by both scientists and managers (Sutula et al., 2015). Our goals were to: (1) determine relationships DO, HAB occurrences, and algal toxins to *chl-a*; and (2) quantify *chl-a* thresholds and associated uncertainties using statistical approaches that identify "protected" and "at risk" categories in the context of WQC for DO and HAB alerts.

Materials and Methods

Study Area

SFB is the largest estuary in California, consisting of several major sub-embayments (Nichols et al., 1986). The estuary receives nutrient loads from 37 publicly owned wastewater treatment works (POTW) serving the area's population of 7.2 million (Fig. 1). Most POTW perform only secondary treatment without additional nitrogen (N) or phosphorus (P) removal. Freshwater flow into SFB comes from two major sources, the Sacramento and San Joaquin Rivers, large rivers that drain 40% of California's landscape. Intense agriculture in the heavily farmed Central Valley combined with urban sources such as Sacramento ~100 km upstream of Suisun Bay (SUB) contribute to high nutrient loads entering the northern estuary from the Sacramento/San Joaquin Delta. Storm-water runoff from densely populated urban areas surrounding SFB also contributes significant nutrients.

Conceptual Approach

Long-term data from the SFB Research Program (1993-2014) of the US Geological Survey (USGS) and concurrent measurements of algal toxins (2012-2014) supported analyses of trends for DO and HAB. Relationships of DO and HAB to *chl-a* were used to identify *chl-a* thresholds that correspond to risks of low DO or HAB alerts. Increased *chl-a* does not uniformly correspond to increased HAB occurrences, particularly for a single phytoplankton species or toxin, and both high-biomass and high-toxicity events are well described (Anderson et al., 2012). For the former, significant relationships between HAB and *chl-a* have been used to support WQC (Shutler et al., 2012; Schaeffer et al., 2012; Harding et al., 2014). Predominance of a particular taxonomic group, i.e., diatoms, expressed as cell counts or fraction of bio-volume is often accompanied by increased *chl-a*. Conditions that support increased *chl-a*, however, are known to increase abundance of the entire phytoplankton community, not just HAB species (Barber and Hiscock, 2006). For our analyses, we assumed increased *chl-a* reflected increased abundance of all phytoplankton, including potentially toxic HAB based on previous studies (Bricker et al., 2008; Glibert et al., 2005).

Decomposition of excess phytoplankton biomass supports DO consumption, leading to hypoxia (DO < 2.8 mg L^{-1}) in stratified conditions. Spatial and temporal displacement of high *chl-a* and DO depletion commonly occurs in estuaries (Rabalais et al., 2014), reflecting strong seasonality of production and consumption (e.g., Wheeler et al., 2003). Empirical relationships between DO and *chl-a* exhibit time lags, with analyses requiring consideration of relevant time and space scales for individual ecosystems. Accordingly, we aggregated DO and *chl-a* data for a range of time scales for the six sub-embayments to evaluate the strength of these relationships.

Data Sources

USGS SFB Research Program. Our analyses drew on time-series data collected on regular cruises by the USGS along a 145-km transect from 1993 – 2014. These observations provided a complete record of *chl-a*, DO, conductivity, temperature, turbidity, and photosynthetically available radiation (PAR) (http://sfbay.wr.usgs.gov/access/wqdata/query/index.html). Vertical profiles were conducted with a Seabird Electronics SBE9+ CTD and rosette sampler equipped with a Turner Designs C3 fluorometer, Li-Cor LI 192 transmissometer, and Seabird SBE 43 DO electrode. Concurrent grab samples were collected for identification and enumeration of phytoplankton species. Discrete measurements of DO and *chl-a* were used to calibrate instruments and correct for turbidity.

Data were aggregated by sub-embayment (Fig. 1) as geomorphology and nutrient loadings affect ecological responses to nutrient inputs in SFB (Jassby et al., 1997). Sub-embayments consist of: (1) Lower South Bay (LSB), the area south of Dumbarton Bridge; (2) South Bay (SB), from Dumbarton Bridge to San Bruno Shoal; (3) Central Bay (CB), from San Bruno Shoal to Angel Island; (4) North Central Bay (NCB), from Angel Island to Pt. San Pablo; (5) San Pablo Bay (SPB), from Pt. San Pablo to Martinez; and (6) Suisun Bay (SUB), east of Martinez. USGS stations corresponding to these sub-embayments are 34-36, 24-32, 23-20, 18-16, 15-10, and 4-8, respectively. For some analyses, data from several sub-embayments were combined based on the statistical similarities to obtain bay-wide metrics, and to increase sample sizes for uncommon, but potentially deleterious HAB species.

HAB Species and Toxins. HAB species identified by the USGS were used for this analysis (Table 1). Seasonal and inter-annual patterns were identified for the three most common HAB species in SFB, *Pseudo-nitzschia sp.*, *Alexandrium sp.*, *Dinophysis sp.*, for several dinoflagellate

145 species, including *Heterosigma akashiwo*, *Karenia mikimotoi*, *Karlodinium veneficum*, and for
146 cyanobacteria including the genera *Microcystis, Oscillatoria, Planktothrix, Anabaenopsis*, and
147 *Anabaena*. Some rare species with low frequencies-of-occurrence were excluded from the
148 analyses. SFB does not currently have established guidance for potentially deleterious HABs, so
149 we used alert levels from the literature, monitoring programs, and analyses of available data.
150 These included: 10^6 cells L^{-1} for cyanobacteria (WHO 2003), presence/absence for *Alexandrium*
151 (http://www.scotland.gov.uk/Publications/2011/03/ 16182005/37), 10^2 - 10^3 cells L^{-1} for
152 *Dinophysis spp.* (http://www.scotland.gov.uk /Publications/2011/03/16182005/37; Vlamis et al.,
153 2014), and 10^5 – 5 x10^5 cells L^{-1} for *Pseudo-nitzschia.* The dinoflagellates *H. akashiwo, K.*
154 *mikimotoi*, and *K. veneficum* lack guidance on alert levels, so we used 5 x 10^5 cells L^{-1} based on
155 expert opinion. No defined alert levels exist for toxin concentrations estimated using Solid Phase
156 Adsorption Toxin-Tracking (SPATT - MacKenzie et al., 2004), thus alert levels were defined as
157 1 ng g^{-1} for microcystins (MCY), and 75 ng g^{-1} for domoic acid (DA) based on laboratory
158 calibrations and studies at the Santa Cruz Municipal Wharf and Pinto Lake, California (Lane et
159 al., 2010; Kudela, 2011; Gibble and Kudela, 2014).
160 We deployed SPATT samplers in the flow-through system of the *R/V Polaris* (~1 m intake)
161 from October 2011 to November 2014 to assess the presence of DA and MCY. Individual
162 SPATT deployments encompassed South SFB (stations 36-18, representing LSB+SB+CB), and
163 typically stations 36-24 for full-bay cruises (representing LSB+SB), NCB (stations 21-16), SPB
164 (stations 15-9), and SUB and the Delta (stations 8-657). Data were binned by sub-embayment,
165 with SB and South-CB defined as stations 36-24 and 36-18, respectively. SPATT were operated
166 as described previously (Lane et al., 2010; Kudela, 2011; Gibble and Kudela, 2014) for MCY,
167 and reported as the total of LR, RR, YR, and LA congeners and domoic acid (DA). SPATT toxin

concentrations were reported in units of ng toxin g^{-1} resin, and represented a weighted-average for the length of deployment (sub-embayment).

Statistical Analyses

Three statistical approaches were used: (1) seasonal Mann-Kendall Test to quantify temporal trends of DO, HAB and *chl-a*; (2) ordinary least squares regressioin (OLS), robust (e.g., Least Absolute Deviation - LAD), and quantile regression to determine relationships of DO, HAB, and *chl-a*; and (3) quantile regression and conditional probability analyses (CPA) to derive quantitative thresholds for *chl-a* based on a failure to achieve DO benchmarks, or an increased risk of reaching HAB abundances to trigger HAB alerts. Quantile regression was used to determine the 10^{th} and 50^{th} (median) quantiles of DO or HAB cell densities conditional on *chl-a*. Quantile regression is statistically analogous to rank-based correlation; it is based on ordering the observations, is robust to extreme values, and does not require assumptions about distributions of residuals (Cade and Noon, 2003). LAD regression is similar to quantile regression when the median quantile is used, although LAD uses ranks. CPA was used to analyze risk of DO below a WQC, or HAB abundance above a set alert level based on *chl-a* $\geq$ a specified concentration (R package *CProb;* Hollister et al., 2008). The baseline probability is the overall probability of exceedance among all observations, without regard to *chl-a* (i.e., *chl-a* > minimum value). Inflection points in the relationship are interpreted as *chl-a* above which probability of an adverse DO or HAB event increases at a faster rate relative to increases of *chl-a*. A probability of 0.5 is nominally defined as a benchmark of "elevated risk" because above this level, an adverse event is more likely to occur than not.

Statistical Analyses of HAB – *Chl-a.* HAB cell densities and toxins were analyzed in the context of seasonal and inter-annual patterns of *chl-a*. Near-surface samples ($\leq$ 2 m) collected

191 from April - November were used for these analyses. "Calculated *chl-a*" consisting of
192 fluorescence calibrated by discrete samples was also used for these analyses. All cell counts for
193 known HAB species were used, regardless of depth or location, to increase sample sizes. More
194 than 95% of HAB were from near-surface samples. USGS enumerates phytoplankton for
195 samples with *chl-a* $\geq$ 5 mg m^{-3}, introducing a possible sampling bias by neglecting HAB at low
196 *chl-a*. Another potential bias in the data is a lack of records for *Microcystis* spp., suggesting these
197 cells were not identified by microscopy although they are regularly observed in northern SFB.

198 OLS and LAD regressions of HAB cell counts and SPATT toxin concentrations on *chl-a*
199 were based on log-transformed data to improve normality. For toxin analysis, $\log_{10}$-transformed
200 SPATT were compared to mean or maximum *chl-a* from corresponding SFB sub-embayments.
201 Cell counts and *chl-a* were transformed by natural logarithm. HAB alert levels (see above) were
202 used to derive probabilities that HAB or toxins would reach problematic levels with increased
203 *chl-a*. Selection of alert level influenced the probability derived from CPA (see below).

204 Quantile regression and CPA were used to identify *chl-a* thresholds based on the risk of
205 exceedances of HAB cell densities or toxin alert levels. First, CPA was conducted on HAB cell
206 densities and SPATT data aggregated for all sub-embayments. A "HAB event of concern" was
207 classified as a site with at least one HAB species exceeding cell-density alert levels. Second,
208 quantile and OLS regressions were used to quantify relationships between cell densities of
209 *Alexandrium*, *Dinophysis*, *Heterosigma*, *Karlodinium*, and *Pseudo-nitzschia* and *chl-a*.
210 Corresponding analyses were performed for SPATT data aggregated among years and sub-
211 embayments. Additional analyses were conducted by sub-embayment, but the results were
212 similar (albeit with reduced statistical power) and were omitted for brevity. Analyses were also
213 performed with and without *Alexandrium*, potentially biasing the analysis because this HAB has

214 a low alert level. Concern that patterns may be strongly influenced by exchange with the open
215 coast led to CPA on the complete time-series stratified by sub-embayment. Finally, data were
216 divided into pre- and post-2002 to identify potential decadal differences.

217 Statistical Analyses of DO - *Chl-a*. Relationships between DO and *chl-a* were derived using
218 the USGS data (1993-2014). Mean *chl-a* from depths ≤ 2 m was calculated for each station for
219 periods-of-interest identified in previous analyses as showing *chl-a* changes (Cloern et al., 2007).
220 These periods include: 1) spring bloom (February-May), 2) summer baseline (June-September),
221 and 3) combination of these two periods (February-September). Mean February-September *chl-a*
222 proved integrative of changing phytoplankton productivity in SFB and was chosen as the time
223 period to derive thresholds of risk of low DO.

224 The evaluation period for DO was based on periods of non-compliance using existing WQC
225 for DO in SFB: 1) an instantaneous WQC > 7 mg L^{-1} upstream and > 5 mg L^{-1} downstream of
226 the Carquinez Bridge, not to fall below these values more than 10% of the time (SFRWQCB,
227 2011); and 2) > 80% saturation in running three-month medians in any sub-embayment of SFB.
228 Medians for percent saturation and concentration (mg L^{-1}) of DO were computed from vertical
229 profiles at each station. The number of stations below the WQC was tabulated by sub-
230 embayment over the 20-year period. The three-month intervals with the most DO exceedances
231 were used for further statistical analyses as these periods are sensitive to low DO and would
232 correspond to protective thresholds for *chl-a*.

233 Quantile regression was used to investigate relationships between DO and *chl-a* by sub-
234 embayment for several time lags. DO percent saturation was preferred to DO concentration as it
235 removed variability associated with effects of temperature and salinity on solubility. Median
236 (i.e., τ =0.5) quantiles of percent DO saturation were used to test the significance and slope of the

relationship between DO and *chl-a* for three periods of integration. Sub-embayments for which a there was a positive slope between median percent DO saturation and *chl-a* were omitted from further analyses.

For sub-embayments with significant ($p < 0.05$) negative relationships between DO and *chl-a*, thresholds of increased risk of falling below DO benchmarks were quantified using two approaches. First, quantile regression using $\tau = 0.1$ was used to predict the mean and 95% confidence intervals of *chl-a* at which a gradient of DO percent saturation of 80%, 72%, 57%, and 46% would be attained 90% of the time. The remaining 10% non-attainment corresponds to California State Water Resource Control Board guidance for listing of impaired waters (SWRCB, 2005). These percent DO saturation are equivalent to DO concentrations of 7.0, 6.3, 5.0 and 4.0 mg L^{-1} at mean summer temperature 15^{o} C and salinity 24. Benchmark concentrations of 6.3 and 5.0 mg L^{-1} are the lowest DO concentrations to which salmonid and non-salmonid fish, respectively, can be exposed indefinitely without resulting in > 5% impact to estuarine populations (Bailey et al., 2014). 7.0 and 5.0 mg L^{-1} benchmarks are the established WQC for DO for SFB sub-embayments. In addition, *chl-a* at which DO percent saturation was expected to meet the median three-month percent saturation WQC of 80% for SFB was estimated as the 50th quantile regression line. Finally, CPA was used to identify change points in the probability of DO falling below established WQC for DO with increasing *chl-a*.

Results

HAB Cell Densities and Algal Toxins

HAB species were detected in ~50% of samples and exceeded alert levels in ~35% of samples. Of samples exceeding alert levels, 53% were associated with *Alexandrium,* 11% with *Dinophysis*, and 7% with *Pseudo-nitzschia* (Fig. 2). Few toxic HAB events have been reported

for SFB, but SPATT data confirm common occurrences of toxins DA and MCY (Fig. 3). Of 158 SPATT samplers we deployed, 72% showed detectable MCY and 97% showed detectable DA. Mean concentrations were 0.75 ng g^{-1} for MCY and 57 ng g^{-1} for DA, with ranges of detectable toxin for SPATT from 0.01 - 25.5 ng g^{-1} for MCY and from 1.69 - 1650 ng g^{-1} for DA (Fig. 3a-b).

DO, HAB Cell Densities, Algal Toxins, and Chl-a

Significant decreases of DO and increases of *chl-a* occurred in all sub-embayments from 1993 – 2013 ($p < 0.05$) based on a seasonal Mann-Kendall test (Fig. 4). Particularly notable were increases of summer baseline *chl-a* throughout SFB, with the largest increases in central and southern sub-embayments (Fig. 4). Sen slopes ranged from -0.9 to -1 percent saturation yr^{-1} for DO and from 0.041 to 0.096 mg m^{-3} yr^{-1} for *chl-a*. Cell counts were aggregated for all sub-embayments to increase sample sizes, except for *Pseudo-nitzschia* (n = 166) and *Alexandrium* (n = 261). HAB organisms *Alexandrium,* several cyanobacteria, *Dinophysis, Heterosigma, Karlodinium,* and *Pseudo-nitzschia* showed no significant increases based on Kendall's Tau tests ($p > 0.1$), while *Karenia* showed a significant, positive trend ($p < 0.05$). Cell counts for *Pseudo-nitzschia* or *Alexandrium* analyzed by sub-embayment showed no significant trends (ANCOVA, $p > 0.05$).

The 10^{th} percentile of summer DO ranged from 5.7 – 7.8 mg L^{-1} on south to north transects (Supplemental Material, Table S1 and Fig. S1). DO was > 5 mg L^{-1} from 97.1 to 100% of the time along these transects, with DO > 7 mg L^{-1} in SUB 100% of the time. For most sub-embayments, evaluation periods that most frequently fell below the WQC for DO consisting of a three-month running median of 80% saturation were May-July and June-August (Supplemental Material, Table S2), and these periods were used in quantile regressions.

Relationships of HAB and Chl-a

Relationships of HAB abundance and SPATT toxins to *chl-a* showed considerable scatter. Cell counts of *Alexandrium, Dinophysis, Karlodinium*, and *Pseudo-nitzschia* increased with increasing *chl-a* and slopes of LAD regressions were significant ($p < 0.05$). Slopes and corresponding [R^2] for these HAB were 0.48 [0.25], 0.56 [0.33], 1.4 [0.44], and 0.43 [0.45] respectively. Cyanobacteria, *Heterosigma*, and *Karenia* showed no significant trends. SPATT data analyzed by sub-embayment showed a significant increase of MCY and DA with increasing mean *chl-a*, and a significant increase of DA with maximum *chl-a*.

Relationships of DO and Chl-a

Median DO in May-July and June-August showed similar patterns with consistently negative slopes for SUB, SPB, SB, and LSB, regardless of the evaluation period for *chl-a* (Table 1; Fig. 5). Slopes were generally steepest and most significant for mean February-September *chl-a*. Unlike other sub-embayments, the DO - *chl-a* relationship for SB was relatively insensitive to the evaluation period for *chl-a*, with significant relationships for most combinations. DO - *chl-a* relationships were significant in LSB for several evaluation periods. The June-September mean was only negative and significant in SPB, SB, and LSB, while the February-May mean was only negative and significant when correlated with SB and LSB (Table 1). In contrast, slopes were often positive for CB and NB. Quantile regressions of SUB and SPB, while significant, contained relatively few observations at high *chl-a* (Fig. 5). In addition, NB and CB had insufficient exceedances of WQC for DO to run CPA. For this reason, all sub-embayments except SB and LSB were omitted from further analyses to derive DO-related *chl-a* thresholds.

Thresholds Based on Chl-a

HAB Relationships to *Chl-a*. The baseline probability of HAB occurrences for the full range of *chl-a* was 0.35 - 0.40 (Fig. 6a). Interpretation of this baseline probability is that 35-40% of all samples from 1993-2014 exceeded HAB alert levels based on abundance (cells L^{-1}). A mean probability of 0.5 to exceed HAB alert levels corresponded to *chl-a* > 37.5 mg m^{-3} with an upper 95% confidence interval of 13.5 mg m^{-3}. An inflection point for probability corresponding to increased risk occurred at *chl-a* > 25 mg m^{-3}We repeated this analysis after removing *Alexandrium* to determine if this species with low alert level affected CPA outputs (Fig. 6b). The relationship between HAB abundance and *chl-a* was weaker at higher *chl-a*, but presence/absence of *Alexandrium* did not affect the baseline probability. Setting an *Alexandrium* alert level other than "present" had little effect on CPA outputs as mean abundance was ~8,000 cells L^{-1} (range: 100-290,000 cells L^{-1}), and an alert level of > 1,000 cells L^{-1} gave similar patterns.

The *chl-a* thresholds derived using CPA were consistent with relationships of HAB species to *chl-a* using quantile regressions or LAD, with a 0.50 probability of HAB corresponding to a broad range of *chl-a* from 3.5 - 40 mg m^{-3}. Low-biomass, highly toxic genera such as *Alexandrium* and *Dinophysis* occupied the low end of the *chl-a* range, while high-biomass genera such as *Heterosigma* and *Pseudo-nitzschia* occurred at the other high end. CPA for individual sub-embayments were affected by sample size with limited observations at high *chl-a*, but comparable thresholds were derived using spatially aggregated data. Exceptions included NCB and CB that showed flat relationships with *chl-a* (e.g., Fig. 7). Other sub-embayments showed increased probabilities of HAB occurrences with increasing *chl-a*, exceeding 0.80 at highest *chl-a* in SPB and SB. More than 90% of *chl-a* observations in NB and CB were < 13 mg m^{-3} for

the 20-year record, and only in SB and LSB were *chl-a* commonly > 13 mg m^{-3} (18% and 26%, respectively; Supplemental Materials, Fig. S2).

OLS regressions of SPATT toxin on *chl-a* were not statistically significant, but CPA on toxins and *chl-a* gave similar inflection points as we derived for HAB organisms. The baseline probability for DA began at ~0.35 (i.e., across all *chl-a* levels) and increased to ~0.6 for observations with *chl-a* >13 mg m^{-3} (Fig. 8a). MCY showed a similar pattern, with a baseline probability of ~0.3 (Fig. 8b). Very few SPATT observations exceeded *chl-a* thresholds for HAB alert levels (>13 mg m^{-3}), but an increased probability of exceeding toxin thresholds at *chl-a* > 10 mg m^{-3} was consistent with the probability of exceeding alert levels for HAB abundance based on CPA (Fig. 6a-b).

Thresholds Relating DO to *Chl-a*. Quantile regression of mean *chl-a* from February-September and DO from May-July in SB and LSB showed consistently significant ($p < 0.1$), negative slopes for $\tau = 0.1$ and 0.5 using all three *chl-a* evaluation periods (Table 1). Slopes were slightly steeper and more significant for May-July then for June-August. Based on quantile regressions for SB using DO from May-July, a mean *chl-a* from February - September of 14 mg m^{-3} was associated with a low frequency of DO falling below the WQC for DO, while the likelihood was higher at *chl-a* of 17 mg m^{-3} (Table 2). Comparison of predicted *chl-a* values for a gradient of DO is instructive. At *chl-a* of 14 mg m^{-3}, 90% of DO observations were predicted to exceed 7 mg L^{-1}, while at *chl-a* of 42 mg m^{-3}, 90% of DO observations were predicted to exceed 5.0 mg L^{-1} (Table 2). For context, the February-September *chl-a* measured at SB sites was below 14 mg m^{-3} 95% of the time over the 20-year record (supplemental materials, Fig. S2).

DO in LSB was predicted to fall below DO benchmarks at lower *chl-a* than in SB, althought confidence intervals were larger. At a mean *chl-a* from February-September of 16 mg m^{-3}, there

was an elevated risk of falling below WQC for DO based on the three-month median for percent saturation (Table 2). A 10% probability of exceeding the WQC for DO was associated with *chl-a* of 4 mg m^{-3}, with a negative lower 95th CI. This suggests advection of DO-depleted water into the study area such that even at extremely low values of *chl-a*, the probability of falling below the WQC for DO is high. Similarly, the CPA showed a baseline probability of 0.2 for falling below the WQC for DO (Fig. 9). This baseline was moderately high considering a mean probability of 0.5 based on the WQC for DO to *chl-a* > 14 mg m^{-3} with an upper 95% confidence interval of > 10 mg m^{-3}. We interpret this result to mean *chl-a* at or above these thresholds entails increased risk of DO below the WQC for DO of 80% saturation with increased *chl-a* (Fig. 9). Applying the CPA and comparing results to DO and *chl-a* distributions in SFB, we observed that 90% of DO values would exceed 6.3 mg L^{-1} and 5.0 mg L^{-1}, respectively, at *chl-a* of 15 mg m^{-3} and 36 mg m^{-3} (Table 2). Long-term data for 20 years showed 95% of *chl-a* measured in LSB was < 25 mg m^{-3} (Supplemental Materials, Fig. S2), and hypoxia associated with high *chl-a* remains uncommon in the open channel habitat of LSB.

Discussion

Current Status and Potential for Eutrophication in SFB

Humans have enriched the world's bays and estuaries with nitrogen and phosphorus, but the responses to enrichment vary widely across ecosystems (Cloern, 2001). Nutrient supply sets the potential for environmental degradation through excess production of algal biomass, but the realization of that potential – i.e., the efficiency with which exogenous nutrients are converted into biomass – depends on factors that regulate phytoplankton population growth, including light availability, toxins, grazing, pathogens, and transport processes. Nutrient concentrations in SFB exceed those that have led to degradation of water quality in other estuaries, but its

phytoplankton biomass (mean *chl-a* concentration) is lower and DO concentrations higher than for other enriched estuaries such Chesapeake Bay, Neuse Estuary, Seine Bay, and the Westerschelde (Bricker et al., 2007; Cloern and Jassby 2008, Fig. 1). However, estuaries are highly dynamic ecosystems that exhibit complex responses to human disturbances, climate variability, and climate change (Cloern et al., 2015, Harding et al., 2015). Changes in SFB during the past two decades include significant increases of *chl-a*, ubiquitous presence of HAB species known to be toxic in other nutrient-enriched estuaries, and significant decreasing trends of DO.

HAB cell densities exceeded alert levels in ~35% of samples from SFB, indicating the potential for adverse effects on ecosystem health. HAB species are expected to occur at some baseline level, based on the cosmopolitan distributions of many species (Lundholm and Moestrop, 2006). However, the probability of a HAB event is high, once seeded, due to nutrient over-enrichment that characterizes SFB. The high baseline of occurrence documented in this study reflects strong connectivity with at least two documented sources of HAB seed populations. The first is the coastal ocean adjacent to SFB, a source of toxic phytoplankton species that lead to closures of shellfish harvesting half the year because of potential exceedances of alert levels based on HAB abundance (Lewitus et al., 2012). The second source is the South Bay salt ponds where the presence of dinoflagellates, *Alexandrium* spp. and *Karenia mikimotoi*, the raphidophyte, *Chattonella marina*, and the cyanophytes, *Anabaenopsis* spp. and *Anabaena* spp. has been confirmed (Thébault et al., 2008). Samples from SB contained other HAB species that were rare in SFB prior to the opening of the Salt Ponds, including *Karlodinium veneficum*, *Chattonella marina*, and *Heterosigma akashiwo*, while abundances of *K. mikimotoi* and *K. veneficum* in LSB and SB increased after breaching of the Salt Ponds. Distributions of these

species show a spatial pattern reveal expansion into the rest of the SFB, suggesting that they pose an emerging threat.

While presence of HAB species above a defined alert level indicates a potential threat, the presence of toxins elevates that threat considerably as it demonstrates that environmental conditions within SFB or connected habitats are conducive to toxin production. SFB is not routinely monitored for algal toxins and no acute wildlife mortalities or human illnesses have been directly attributed to HAB from 1993-2014. MCY in SFB, however, has been linked to negative impacts on aquatic food webs (Lehman et al., 2010), and there is increasing evidence that chronic, sub-lethal exposure to DA constitutes a significant impairment (Goldstein et al., 2008; Montie et al., 2012). *Pseudo-nitzschia* exceeded alert levels in only 11% of samples, and cyanobacteria cells were not recorded, nonetheless, 72% and 96% of SPATT showed measurable quantities of the toxins MCY and DA, respectively. SPATT detects low concentrations of toxins compared to traditional methods (Lane et al., 2010; Kudela, 2011), and removal of SPATT data with the lowest toxin levels still left ~35% of samples with toxin levels of concern. These findings suggest that dissolved toxins are widely distributed in SFB. SPATT were not analyzed for other toxins that may occur in SFB, and the threat of HAB toxins remains requires further study.

Significant relationships of HAB abundance to *chl-a* were detected in SFB, while low DO and high *chl*-a were rarely observed and relationships differed by sub-embayment. In Northern SFB, DO was high and relatively low *chl-a* accompany depressed primary production with several possible causes, including inhibition and grazing (Dugdale et al., 2007; Cloern et al., 2014). The lack of consistent, significant relationships between DO and *chl-a* in SUB, SPB and CB sub-embayments suggests that physical processes, such as strong tidal mixing and a lack of

418 persistent stratification, partially alleviate the development of low DO, despite high
419 phytoplankton biomass (Smith and Hollibaugh, 2006). These modulating factors appear
420 important in both CB and SUB, sub-embayments that are adjacent to the coastal ocean and the
421 Sacramento/San Joaquin Delta, respectively. In contrast to CB and SUB sub-embayments, DO
422 was lowest and *chl-a* was highest in LSB, a lagoonal sub-embayment with a long residence time
423 that is near productive intertidal habitats that experience hypoxia, such as the restored salt ponds
424 in SB (Thebault et al., 2008) and tidal sloughs (Senn et al., 2014).

425 SFB is responsive to both climate forcing and climate change (Cloern et al., 2015), and these
426 factors can lead to shifts in the efficiency of nutrient assimilation into phytoplankton biomass, as
427 reported for the Baltic Sea (Riemann et al., 2015). The high ambient nutrient concentrations that
428 characterize SFB suggest a potential for accumulation of phytoplankton biomass sufficient to
429 impair water quality. To evaluate this potential, we computed median concentrations of dissolved
430 inorganic nitrogen (DIN) and *chl-a* for four sub-embayments (Table 3). We then estimated
431 potential *chl-a* as the sum of measured *chl-a* plus the amount of *chl-a* that would be produced if
432 all remaining DIN was assimilated into phytoplankton biomass, assuming a conversion factor of
433 1 g *chl-a* per mol N (Eppley et al., 1971). We found median *chl-a* in all sub-embayments of SFB
434 would increase an order of magnitude if this potential was realized. Given uncertainty about the
435 future trajectory of water quality in SFB, a potential for increased phytoplankton biomass
436 justifies establishment of *chl-a* thresholds to support nutrient management directed at reducing
437 risk of impairments.

438

439 *Chl-a as the Basis to Assess Water-Quality Impairments*

Chl-a is an integrative measure of water quality that has been used to assess eutrophication in estuaries around the world (Bricker et al., 2003; Zaldivar et al., 2008). Our analyses have related specific water-quality impairments in SFB to *chl-a*, consistent with published work that applies *chl-a* as a pivotal indicator of nutrient over-enrichment. We present several key findings that support this approach. First, we documented significant relationships between HAB abundance, DO and *chl-a* using quantile regressions. Our results are consistent with a conceptual model of increased risk for HAB abundance, toxins, and low DO at increased phytoplankton biomass (Cloern, 2001). Second, several statistical approaches yield consistent ranges for chl-a threshold based on HAB and DO. An inflection point at mean monthly *chl-a* < 13 mg m^{-3} was a threshold below which the probability of potentially deleterious conditions quantified by HAB abundance and SPATT-derived toxins decreased. This *chl-a* threshold was similar to mean seasonal *chl-a* of 13 - 16 mg m^{-3} associated with attainment of the WQC for DO in SFB, based on the three-month median percent saturation of 7 mg L^{-1}. At the opposite end of the risk continuum, inflection points of heightened risk of HAB cell density (*chl-a* from 25 - 40 mg m^{-3}) corresponded well to mean seasonal *chl-a* thresholds of 35-40 mg m^{-3} required for LSB and SB to fall more consistently below the 5.0 mg L^{-1} DO WQC. Third, *chl-a* thresholds we derived for SFB were in agreement with published water-quality criteria using a variety of assessment methods. Several examples are consistent with *chl-a* thresholds that we derived for SFB based on relationships with HAB and DO. Harding et al. (2014) reported that mean summer *chl-a* from 7.2 – 11 mg m^{-3} precluded low DO in the deep waters of Chesapeake Bay, and that mean annual *chl-a* of 15 mg m^{-3} was associated with decreased risk of *Microcystis* spp. toxins. Bricker et al. (2003) designated > 20 mg m^{-3} as a threshold of "high" risk for eutrophication, a value agreed upon by expert judgment. Similarly, *chl-a* thresholds of 10, 20 and 50 mg m^{-3} are used to define

463 categories of low, high, and very high risk of eutrophication in the Phytoplankton Biological
464 Quality Element for the European Union (EU) Water Framework Directive (WFD) proposed in
465 the United Kingdom (Devlin et al., 2011).

466

467 *"Risk Assessment" and Uncertainty in Chl-a Thresholds*

468 Environmental management and regulation are firmly grounded in a paradigm of "risk
469 assessment" (US Environmental Protection Agency, 1998). For this reason, risk represents a
470 useful context to express *chl-a* thresholds and uncertainties with respect to WQC for SFB. Here,
471 we used CPA and quantile regression to derive *chl-a* thresholds corresponding to low and high
472 risk of exceeding HAB alert levels. A similar approach is commonly used to derive WQC for
473 freshwater ecosystems, but few applications exist for the marine environment (Paul et al., 2005).
474 Both CPA and quantile regression provide quantitative measures of uncertainty, a key element to
475 support environmental decision-making (National Research Council, 2009).

476 CPA and quantile regression provided estimates of statistical uncertainty for *chl-a* thresholds
477 based on HAB and DO, but other sources of uncertainty should be considered when applying
478 these thresholds to nutrient management. First, the ecological significance of HAB species in
479 SFB is not well known. Data needs include bio-accumulation of particulate and dissolved toxins
480 in the biota, and acute and chronic impairments of ecosystem health. Such efforts should be
481 coupled to an improved understanding of relationships between HAB toxins and *chl-a* specific to
482 each sub-embayment. Second, spatial and temporal dynamics of low summer DO and seasonal
483 maxima of *chl-a* that support DO consumption require additional study. Conceptually, it is
484 possible that the mechanism behind this relationship is that high primary production on seasonal
485 to annual time scales is expected to promote increased abundance of detritus, which, during the

summer, leads to an increased probability of net ecosystem heterotrophy (Caffrey, 2003). Large spring blooms and subsequent fall blooms that were prominent features of the annual phytoplankton cycle in 2000 (Cloern et al., 2007) have not occurred in the past five years; in contrast, the summertime baseline that has seen the largest magnitude increase from 1993 to 2014 (Fig. 4). In-depth investigations into phytoplankton contribution to the SFB carbon budget and its relative influence on the coupling of pelagic and benthic metabolism are needed to better understand the relationships behind these empirical relationships between DO and *chl-a* in SB and LSB (e.g., Murrell et al., 2013).

Finally, there is a need to review the relevance and adequacy of scientific data supporting WQC for DO in SFB, specifically in LSB. Over the last 20 years, LSB has met 5.7 mg L^{-1}, the benchmark proposed by Best et al. (2007) that corresponds to the highest ecological condition category in EU estuaries. However, it has frequently not met the WQC based on three-month median percent DO saturation of > 80%, a value that at mean summer salinities and temperatures is equivalent to 7 mg L^{-1}. The question is whether 7 mg L^{-1} is a reasonable expectation for DO in LSB, given that this sub-embayment is strongly influenced by highly productive, intertidal habitats (Thebault et al., 2008; Shellenbarger et al., 2008).

Such investigations should be nested within an improved monitoring program, as the complexity of these patterns remind us that SFB is in a continuing state of change, one that is likely to continue over the next century (Cloern et al., 2011). Although it is attractive to consider relationships of impairments such as HAB abundance and low DO to *chl-a* as constant, we recognize that *chl-a* thresholds are responsive to changes in fundamental drivers of phytoplankton dynamics, such as oceanic exchange, top-down grazing, and light limitation. Changes in the relationships of impairments to *chl-a* will almost certainly respond to climate

variability and climate change, as reported for this and other ecosystems (Cloern et al., 2014; Riemann et al., 2015).

Summary

This study demonstrated that, while DO is higher and *chl-a* lower in SFB than in other estuaries subject to nutrient over-enrichment, this important ecosystem is poised to express symptoms of cultural eutrophication. We found that evidence of ubiquitous HAB abundance, HAB toxins, declining DO, and increasing *chl-a*, supporting generalized conceptual models that describe increased risk of HAB cell densities and toxin concentrations and declining DO with increasing phytoplankton biomass. The majority of SFB subembayments are currently below *chl-a* < 13 mg m^{-3}, representative of baseline probabilities of HAB occurrence and attainment of SFB's 3-month median percent saturation DO WQC. However, SFB has sufficient dissolved inorganic nutrients to reach chl-a levels defined by "high risk" thresholds in the range of 25-40 mg m-3 *chl-a*, suggesting a potential for increased biomass accumulation that could lead to cultural eutrophication. Given the uncertainty in SFB's trajectory amidst global change, it is this potential for high biomass production that motivates establishment of *chl-a* water quality goals to support nutrient management of SFB, and underlines the need for continued monitoring of SFB to understand how these fundamental relationships may change in the future.

Acknowledgements

Funding for this study was provided through a contract with the San Francisco Water Quality Control Board (11-151-120). This work benefited from many discussions with the SFB Nutrient Technical Workgroup and Steering Committee.

References

Andersen, J. H., Murray, C., Kaartokallio, H., Axe, P., Molvær, J., 2010. Confidence rating of eutrophication status classification. Mar. Pollut. Bull. 60, 919–924.

Andersen, J. H., Carstensen, J., Conley, D. J., Dromph, K., Fleming-Lehtinen, V., Gustafsson, B.G., Josefson, A.B., Norkko, A., Villnas, A., Murray, C., 2015. Long-term temporal and spatial trends in eutrophication status of the Baltic Sea. Biol. Rev. doi: 10.1111/brv.12221

Anderson, D. M., Cembella, A. D., Hallegraeff, G. M., 2012. Progress in understanding harmful algal blooms: paradigm shifts and new technologies for research, monitoring, and management. Ann. Rev. Mar. Sci., 4, 143-176.

Bailey, H., Curran, C., Poucher, S., Sutula, M., 2014. Science supporting dissolved oxygen objectives for Suisun Marsh. Southern California Coastal Water Research Project Authority Technical Report 830. www.sccwrp.org. 33 p.

Barber, R. T., Hiscock, M. R., 2006. A rising tide lifts all phytoplankton: Growth response of other phytoplankton taxa in diatom-dominated blooms. Global Biogeochem. Cycles 20, GB4S03, doi:10.1029/2006GB002726.

Baustian, M. M., Rabalais, N. N., 2009. Seasonal composition of benthic macroinfauna exposed to hypoxia in the Northern Gulf of Mexico. Estuar. Coasts 32, 975-983.

Best, M. A., Wither, A. W., Coates, S., 2007. Dissolved oxygen as a physico-chemical supporting element in the Water Framework Directive, Mar. Pollut. Bull. 55, 53-64.

Bricker, S. B., Ferreira, J. G., Simas, T., 2003. An integrated methodology for assessment of estuarine trophic status. Ecol. Modell. 169, 39-60.

552 Bricker, S., Longstaff, B., Dennison, W., Jones, A., Boicourt, C., Wicks, C., Woerner, J., 2007.
553 Effects of nutrient enrichment in the Nation's estuaries: a decade of change. NOAA Coastal
554 Ocean Program Decision Analysis Series No. 26. National Centers for Coastal Ocean
555 Science, Silver Spring, Maryland, USA. 328 p.

556 Cade, B. S., Noon, B. R., 2003. A gentle introduction to quantile regression for ecologists. Front.
557 Ecol. Environ. 1, 412-420.

558 Caffrey, J. M., 2003. Production, respiration and net ecosystem metabolism in US estuaries.
559 Environ. Mon. Assess. 81, 207-219.

560 Cloern, J. E., 2001. Our evolving conceptual model of the coastal eutrophication problem. Mar.
561 Ecol. Prog. Ser. 210, 223-253.

562 Cloern, J. E., Cole, B. E., Hager, S. W., 1994. Notes on *Mesodinium rubrum* red tides in San
563 Francisco Bay (California, USA). J. Plankton Res. 16, 1269–1276.

564 Cloern, J. E., Dufford, R., 2005. Phytoplankton community ecology: principles applied in San
565 Francisco Bay. Mar. Ecol. Prog. Ser. 285, 11-28.

566 Cloern, J. E., Schraga, T. S., Lopez, C. B., Knowles, N., Labiosa, R. G., Dugdale, R., 2005.
567 Climate anomalies generate an exceptional dinoflagellate bloom in San Francisco Bay.
568 Geophys. Res. Lett. 32, L14608, doi:10.1029/2005GL023321.

569 Cloern, J., Jassby, A., Thompson, J., Hieb, K., 2007. A cold phase of the East Pacific triggers
570 new phytoplankton blooms in San Francisco Bay. Proc. Natl. Acad. Sci. U.S.A. 104, 18,561-
571 18,565.

572 Cloern, J. E., Jassby, A., 2008. Complex seasonal patterns of primary producers at the land-sea
573 interface. Ecol. Lett. 11, 1294-303. doi: 10.1111/j.1461-0248.2008.01244.

574 Cloern, J. E., Knowles, N., Brown, L. R., Cayan, D., Dettinger, M. D., Morgan T. L.,
575 Schoellhamer, D. H., Stacey, M. T., van der Wegen, M., Wagner, R. W., Jassby, A., 2011.
576 Projected Evolution of California's San Francisco Bay-Delta-River System in a Century of
577 Climate Change. PLoS ONE 6, e24465. doi:10.1371/journal.pone.0024465

578 Cloern, J. E., Jassby, A. D., 2012. Drivers of change in estuarine-coastal ecosystems: discoveries
579 from four decades of study in San Francisco Bay. Rev. Geophys. 50, RG4001,
580 doi:10.1029/2012RG000397.

581 Cloern, J. E., Foster, S. Q., Kleckner, A. E., 2014. Phytoplankton primary production in the
582 world's estuarine-coastal ecosystems. Biogeosciences 11, 2477–2501. doi:10.5194/bg-11-
583 2477-2014

584 Cloern, J. E., Abreu, P. C., Carstensen, J., Chauvaud, L., Elmgren, R., Grall, J., Greening, H.,
585 Johansson, J. O. R., Kahru, M., Sherwood, E. T., Xu, J., Yin, K., 2015. Human activities and
586 climate variability drive fast-paced change across the world's estuarine-coastal ecosystems.
587 Glob. Chang. Biol. doi:10.1111/gcb.13059

588 Devlin, M., Bricker, S., Painting, S., 2011. Comparison of five methods for assessing impacts of
589 nutrient enrichment using estuarine case studies, Biogeochemistry 106, 177-205.

590 Diaz, R. J., Rosenberg, R., 1995. Marine benthic hypoxia: a review of its ecological effects and
591 the behavioral responses of benthic macrofauna. Oceanogr. Mar. Biol. Ann. Rev. 33, 245-
592 303.

593 Diaz, R. J., Rosenberg, R., 2008. Spreading dead zones and consequences for marine
594 ecosystems, Science 321, 926–929.

595 Dugdale, R. C., Wilkerson, F. P., Hogue, V. E., Marchi, A., 2007. The role of ammonium and
596 nitrate in spring bloom development in San Francisco Bay. Estuar. Coast. Shelf Sci. 73, 17-
597 29.

598 Eppley, R. W., Carlucci, A. F., Holm-Hansen, O., Kiefer, D., McCarthy, J. J., Venrick, E.,
599 Williams, P. M., 1971. Phytoplankton growth and composition in shipboard cultures supplied
600 with nitrate, ammonium, or urea as the nitrogen source. Limnol. Oceanogr. 16, 741-751.

601 Gibble, C., Kudela, R., 2014. Detection of persistent microcystins toxins at the land-sea interface
602 in Monterey Bay, California. Harmful Algae 39, 146-153. doi:10.1016/j.hal.2014.07.004

603 Glibert, P. M., Anderson, D. M., Gentien, P., Graneli, E., Sellner, K. G., 2005. The global,
604 complex phenomena of harmful algal blooms. Oceanography 18, 137–147.

605 Goldstein, T., Mazet, J. A. K., Zabka, T. S., Langlois, G., Colegrove, K. M., Silver, M., Bargu,
606 S., Van Dolah, F., Leighfield, T., Conrad, P. A., Barakos, J., Williams, D. C., Dennison, S.,
607 Haulena, M., Gulland, F. M. D., 2008. Novel symptomatology and changing epidemiology of
608 domoic acid toxicosis in California sea lions *Zalophus californianus*: an increasing risk to
609 marine mammal health. Proc. Royal Soc. B: Biol. Sci. 275, 267-276.

610 Harding, L. W., Jr., Batiuk, R. A., Fisher, T. R., Gallegos, C. L., Malone, T. C., Miller, W. D.,
611 Mulholland, M. R., Paerl, H. W., Perry, E. S., Tango, P., 2014. Scientific bases for numerical
612 chl-a criteria in Chesapeake Bay. Estuar. Coasts 37, 134-148.

613 Harding, L. W., Jr., Gallegos, C. L., Perry, E. S., Miller, W. D., Adolf, J. E., Mallonee, M. E.,
614 Paerl, H. W., 2015. Long-term trends of nutrients and phytoplankton in Chesapeake Bay.
615 Estuar. Coasts. doi:10.1007/sl2237-015-0023-7.

Heisler, J., Glibert, P. M., Burkholder, J. M., Anderson, D. M., Cochlan, W., Dennison, W. C., Dortch, Q., Gobler, C. H., Heil, C. A., Humphries, E., Lewitus, A., Magnien, R., Marshall, H. G., Sellner, K. G., Stockwell, D. A., Suddleson, M., 2008. Eutrophication and harmful algal blooms: a scientific consensus. Harmful Algae 8, 3-13.

Hollister J., Walker, H., Paul, J. F., 2008. CProb: A computational tool for conducting conditional probability analysis. J. Environ. Qual. 37, 2392-2396.

Jassby, A.D., Cole, B. E., Cloern, J. E., 1997. The design of sampling transects for characterizing water quality in estuaries. Estuar. Coast. Shelf Sci. 45, 285–302.

Kimmerer, W. J., Thompson J. K., 2014. Phytoplankton growth balanced by clam and zooplankton grazing and net transport into the low-salinity zone of the San Francisco Estuary. Estuar. Coasts 37, 1202-1218.

Kirkpatrick, B., Fleming, L. E., Squicciarini, D., Backer, L. C., Clark, R., Abraham, W., Benson, J., Cheng, Y. S., Johnson, D., Pierce, R., Zaias, J., Bossart, G., Baden, D. G., 2004. Literature review of Florida red tide: Implications for human health effects. Harmful Algae 3, 99–115.

Kudela, R. M., 2011. Characterization and deployment of Solid Phase Adsorption Toxin Tracking (SPATT) resin for monitoring of microcystins in fresh and saltwater. Harmful Algae 11, 117-125.

Lane, J. Q., Roddam, C. M., Langlois, G. W., Kudela, R. M., 2010. Application of Solid Phase Adsorption Toxin Tracking (SPATT) for field detection of domoic acid and saxitoxin in coastal California. Limnol. Oceanogr. Methods 8, 645–660.

636 Lehman, P. W., Boyer, G., Hall, C., Waller, S., Gehrts, K., 2005. Distribution and toxicity of a
637 new colonial *Microcystis aeruginosa* bloom in the San Francisco Bay Estuary, California.
638 Hydrobiol. 541, 87-99.

639 Lehman, P. W., Teh, S. J., Boyer, G. L., Nobriga, M., Bass, E., Hogle, C., 2010. Initial impacts
640 of *Microcystis* on the aquatic food web in the San Francisco Estuary. Hydrobiol. 637, 229–
641 248.

642 Lewitus, A. J., Horner, R. A., Caron, D. A., Garcia-Mendoza, E., Hickey, B. M., Hunter, M.,
643 Huppert, D. D., Kudela, R. M., Langlois, G. W., Largier, J. L., 2012. Harmful algal blooms
644 along the North American west coast region: History, trends, causes, and impacts. Harmful
645 Algae 19, 133-159.

646 Lundholm, N, Moestrop, O., 2006. The biogeography of harmful algae. In: Ecology of Harmful
647 Algae (Granelli, E., Turner, J. T. Eds.), Ecological Studies 189, Springer.

648 Mackenzie, L., Beuzenberg, V., Holland, P., Mcnabb, P., Selwood, A., 2004. Solid phase
649 adsorption toxin tracking (SPATT): a new monitoring tool that simulates the biotoxin
650 contamination of filter feeding bivalves. Toxicon 44, 901-918.
651 doi:10.1016/j.toxicon.2004.08.020.

652 Montie, E. W., Wheeler, E., Pussini, N., Battey, T. W. K., Van Bonn, W., Gulland, F., 2012
653 Magnetic resonance imaging reveals that brain atrophy is more severe in older California sea
654 lions with domoic acid toxicosis. Harmful Algae 20, 19-29.

655 Murrell, M. C., Stanley, R., Lehrter, J. C., Hagy, J. D., 2013. Plankton community respiration,
656 net ecosystem metabolism, and oxygen dynamics on the Louisiana continental shelf:
657 Implications for hypoxia, Cont. Shelf Res. 52, 27-37.

Nichols, F. H., Cloern, J. E., Luoma, S. N., Peterson, D. H., 1986. The modification of an estuary. Science 231, 567–573.

Nixon, S. W., 1995. Coastal marine eutrophication: a definition, social causes, and future concerns. Ophelia 41, 199–219.

National Research Council, 2009. Science and decisions: advancing risk assessment. Committee on Improving Risk Analysis Approaches Used by U.S. EPA, Board on Environmental Studies and Toxicology. doi: 10.17226/12209.

Paerl, H. W., 1995. Coastal eutrophication in relation to atmospheric nitrogen deposition: Current perspectives. Ophelia 41, 237-259.

Paul, J. F., McDonald, M. E., 1997. Development of empirical, geographically-specific water quality criteria: a conditional probability analysis approach. J. Am. Water Resour. Assoc. 41, 1211-1223.

Rabalais, N. N., Cai, W. -J., Carstensen, J., Conley, D. J., Fry, B., Hu, X., Quiñones-Rivera, z., Rosenberg, R., Slomp, C. P., Turner, R. E., Voss, M., Wissel, B., Zhang, J., 2014. Eutrophication-driven deoxygenation in the coastal ocean. Oceanography 27, 172–183.

Riemann, B., Carstensen, J., Dahl, K., Fossing, H., Hansen, J. W., Jakobsen, H. H., Josefson, A. A., Krause-Jensen, D., Markager, S., Stæhr, P.A., Timmermann, K., Windolf, J., Andersen, J. H., 2015. Recovery of Danish coastal ecosystems after reductions in nutrient loading: A holistic ecosystem approach. Estuar. Coasts doi: 10.1007/s12237-015-9980-0.

Rosenberg, R., Hellman, B. Johansson, B., 1991. Hypoxic tolerance of marine benthic fauna Mar. Ecol. Prog. Ser. 79, 127-131.

679 Schaeffer, B. A., Hagy, J. D., Conmy, R. N., Lehrter, J. C., Stumpf, R. P., 2012. An approach to
680 developing numeric water quality criteria for coastal waters using the SeaWiFS satellite data
681 record. Environ. Sci. Technol. 46, 916-922.

682 Shellenbarger, G. G., Schoellhamer, D. H., Morgan, T. L., Takekawa, J. Y., Athearn, N. D.,
683 Henderson, K. D., 2008. Dissolved oxygen in Guadalupe Slough and Pond A3W, South San
684 Francisco Bay, California, August and September 2007. U.S. Geological Survey Open-File
685 Report 2008–1097, 26 p.

686 Shutler, J. D., Davidson, K., Miller, P. I., Swan, S. C., Grant, M. G., Bresnan, E., 2012. An
687 adaptive approach to detect high-biomass algal blooms from EO chl-a-*a* data in support of
688 harmful algal bloom monitoring. Rem. Sens. Lett. 3, 101-110.

689 Smith S.V., Hollibaugh, J. T., 2006. Water, salt, and nutrient exchanges in San Francisco Bay.
690 Limnol. Oceanogr. 51, 504–517.

691 State Water Resource Water Quality Control Board (SFRWQCB), 2011. San Francisco Bay
692 Basin (Region 2) Water Quality Control Plan. As amended December 2011, available at
693 www.waterboards.ca.gov/rwqcb2/basin_planning.shtml.

694 Sutula, M., Senn, D., 2016. Scientific bases for assessment of nutrient impacts on San Francisco
695 Bay. Southern California Coastal Water Research Project Authority Technical Report 864.
696 www.sccwrp.org. 56 pp.

697 Tett, P., Gowen, R., Mills, D., Fernandes, T., Gilpin, L., Huxham, M., Kennington, K., Read, P.,
698 Service, M., Wilkinson, M., Malcolm, S., 2007. Defining and detecting undesirable
699 disturbance in the context of marine eutrophication. Mar. Poll. Bull. 55, 282-297.

700 Thébault, J., Schraga, T. S., Cloern, J. E., Dunlavey, E. G., 2008. Primary production and
701 carrying capacity of former salt ponds after reconnection to San Francisco Bay. Wetlands 28,
702 841-851.

703 Topping, B. R., Kuwabara, J.S., Athearn, N.D., Takekawa, J.Y., Parchaso, F., Henderson, K.D.,
704 Piotter, S., 2009. Benthic oxygen demand in three former salt ponds adjacent to south San
705 Francisco Bay, California. U.S. Geological Survey Open-File Report 2009-1180, 21 p.

706 U.S. Environmental Protection Agency, 1998. Guidelines for Ecological Risk Assessment.
707 EPA/630/R-95/002F.

708 Vlamis A. and P. Katikou. 2014. Climate influence on Dinophysis spp. spatial and temporal
709 distributions in Greek coastal water. Plankton Benthos Res 9(1): 15–31.

710 Wheeler, P.A., Huyer, A., Fleischbein, J., 2003. Cold halocline, increased nutrients and higher
711 chl-a off Oregon in 2002. Geophys. Res. Lett. 30, doi: 10.1029/2003GL017395. issn: 0094-
712 8276.

713 Zaldivar, J. M., Viaroli, P., Newton, A., De Wit., R., Ibanez, C., Reizopoulou, S., Somma, F.,
714 Razinkovas, A., Basset, A., Holmer, M., Murray, N., 2008. Eutrophication in transitional
715 waters: an overview, Trans. Waters Mono. 1, 1-78.

716 **Figure Legends**

717 Fig. 1. SFB showing distribution of habitat types and locations of sub-embayments Suisun Bay
718 (SUB), San Pablo Bay (SBP), North Central Bay (NCB), Central Bay (CB), South Bay (SB), and
719 Lower South Bay (LSB), defined by Jassby et al. (1997), relative to the locations of major cities
720 in region.

721 Fig. 2. Time series of major HAB in SFB from 1993-2014. Symbols indicate cell densities (cells
722 mL^{-1}) by cruise. The station with the highest cell density is indicated for cruises with HAB
723 enumerated at multiple locations. Inset values give cell densities at stations > 200 cells mL^{-1}.

724 Fig. 3. Concentration of (a) DA (ng g^{-1}) and (b) MCY (LR, RR, YR, and LA in ng g^{-1}) from
725 SPATT deployed in the R/V *Polaris* surface mapping system for regions representing the
726 following sub-embayments: SUB+ Delta station, SPB, NCB, and SB+CB during full Bay
727 cruises, and LSB+SB during South SFB only cruises sub-embayments. Circles indicate DA (top)
728 or MCY concentrations (bottom); for DA > 400 ng g^{-1} and MCY > 10 ng g^{-1}, and numeric values
729 indicate the concentrations.

730 Fig. 4. Monthly geomean and 95% CI of *chl-a* over the periods from 1993-1999 and 2000-2014,
731 by subembayment, from north to south, (a) SUB, (b) SPB, (c) NCB, (d) CB, (e) SB, and (f) LSB.
732 Comparison of *chl-a* before and after 1999 is important temporal benchmark as Cloern et al.
733 (2007) identified a *chl-a* step change coincident with the shifting of the NE Pacific to its cool
734 phase.

735 Fig. 5. Comparison of quantile regressions relating May-July DO percent saturation to *chl-a* in
736 selected sub-embayments from north to south: (a) SUB, (b) SPB, (c) SB and (d) LSB. Lines for
737 the 10^{th} (τ=0.1, red) and median quantiles (τ=0.5, blue) are shown for the quantile regressions.
738 Results of regression analyses are given in Table 1.

739 Fig. 6. Probability of HAB cell densities higher than alert levels as specified value of *chl-a* is
740 exceeded for data in which (a) all HAB species are included and (b) excluding *Alexandrium*. The
741 black line represents mean probability. Grey dashed lines are lower and upper 95% confidence
742 intervals of bootstrap values (100 iterations).

743 Fig. 7. Mean probability of observing any HAB species at concentrations higher than defined
744 alert levels if specified value of *chl-a* is exceeded, by sub-embayment for CB (open squares), SB
745 (black triangle), and LSB (grey circle).

746 Fig. 8. Probabilities of DA (top panel) or MCY (bottom panel) > 75 ng g^{-1} and 1 ng g^{-1},
747 respectively, indicating risk when specified values of *chl-a* are exceeded. The black line
748 represents mean probability. Dashed lines are lower and upper 95% confidence intervals from
749 bootstrap (100 iterations).

750 Fig. 9. Probability of DO percent saturation < 80% during the months of June-August in LSB as
751 specified value of February – September mean *chl-a* is exceeded. The black line represents mean
752 probability. Grey dashed lines are lower and upper 95% confidence intervals of bootstrap values
753 (100 iterations).

754 **Figure Legends (Supplemental)**

755 Fig. S1. Cumulative frequency distribution of minimum monthly DO by sub-embayment
756 stations.

757 Fig. S2. Cumulative frequency distribution of (left panel) annual calendar mean and February-
758 September *chl-a* for South and Lower South Bays as a proportion of site -years of 1993-2013 and
759 (right panel) monthly *chl-a* by all sub-embayments as a proportion of site-years.

Table 1. Slopes of quantile regressions at Tau= 0.1 and 0.5 by DO integrating period (May-July and June-August) and chlorophyll-a averaging period (February-May, June-September, and February-September mean chlorophyll-a). * designates p< 0.1, ** designates p<0.05 and * designates P< 0.01.**

Subembayment and DO Integrating Period	Slope of Quantile Regressions and Significance Level					
	February-May Mean		June-September Mean		February-September Mean	
	0.1 Tau	0.5 Tau	0.1 Tau	0.5 Tau	0.1 Tau	0.5 Tau
May-July						
Lower South	0.06	-0.04	-0.22	-0.62**	-0.73**	-0.61**
South	-0.38***	-0.28***	-0.17	-0.58***	-0.78***	-0.73***
Central	-0.43	0.01	2.15***	0.74**	-0.73	0.15
North Central	-0.20	0.14	1.18	0.87	-0.84	0.85
San Pablo	-0.36	-0.44	-0.93	-0.58***	-0.77	-0.37
Suisun	-0.85	-0.57	-0.86	-0.45	-1.99***	-0.16
June-August						
Lower South	-0.14	-0.23***	0.62	0.39	-0.14	-0.20
South	-0.29***	-0.17***	0.16	-0.02	-0.60***	-0.39***
Central	-0.47	-0.10	0.74*	0.70**	0.27	0.27
North Central	-0.25	-0.13	0.98	0.60	0.39	0.39

San Pablo	-0.20	-0.11	-0.11	-0.36*	-0.33	-0.33
Suisun	0.02	0.05	-1.08	-0.82	0.49	-0.49

Table 2. Comparison of mean and 95% CI (in parentheses) of predicted *chl-a* (mg m^{-3}) from quantile regressions of February –September mean *chl-a* and May-July DO for specified DO benchmarks. 80% saturation at a τ= 0.5 is equivalent to SFB's percent saturation WQC. Predicted *chl-a* at τ= 0.1 represent a 10% frequency of falling below a gradient of DO benchmarks from the literature (i.e. 80%, 72%, 66% and 57% saturation, with corresponding to DO concentrations at mean summertime temperature of 15ºC and salinity of 24 ppt in SB and LSB). All regressions were significant for p< 0.05 (Table 1).

DO Percent saturation, with Equivalent DO Concentration	Predicted Mean *Chl-a* (95% CI)	
	LSB (N=48)	SB (N=161)
τ= 0.5		
80% (~7 mg L^{-1})	15.6 (9.2 – 21.8)	17.3 (15.1 – 19.5)
τ = 0.1		
80% (~ 7.0 mg L^{-1})	4.3 (-4.1 – 12.1)	14.3 (12.6 – 15.5)
72% (~6.3 mg L^{-1})	15.3 (5.3 – 29.3)	24.6 (21.9 – 24.7)
66% (~5.7 mg L^{-1})	23.5 (15.3 – 39.3)	32.3 (29.5 – 32.3)
57% (~ 5.0 mg L^{-1})	35.8 (30.3 – 54.3)	43.8 (40.5 – 45.9)
46% (~4.0 mg L^{-1})	50.9 (41.4 – 60.4)	57.9 (56.2 – 59.2)

Table 3. Median values of dissolved inorganic nitrogen (DIN), measured *chl-a* concentration, and potential *chl-a* concentration if all DIN was assimilated into additional phytoplankton biomass. Data from the USGS SFB water-quality measurement program for years 2000-2014.

Sub-embayment	DIN (µM)	Measured *Chl-a* (mg m^{-3})	Potential *Chl-a* (mg m^{-3})
SUB	36.9	2.5	39.7
SPB	29.0	3.8	33.6
SB	31.4	5.5	39.2
LSB	57.5	7.5	67.0

SUPPLEMENTAL MATERIALS

Table A1. 10th Percentile of the vertical median and minimum summer (May-August) DO concentration over the period of 1993-2014 and percentage of time over that period that DO concentration was less than 5 mg L^{-1}.

Sub-embayment	10th Percentile of Summer Vertical Median DO (mg L^{-1})	10th Percentile of DO Summer Vertical Minimum (mg L^{-1})	% of Time Summer DO< 5 mg L^{-1}
Lower South Bay	5.7	5.6	2.9
South Bay	5.9	5.8	0.5
Central Bay	6.5	6.5	0.2
North Central Bay	6.8	6.4	1.9
San Pablo Bay	7.1	7	0
Suisun Bay	7.8	7.7	0

Table A4. Percent of site-events that fell below DO objectives of 3 month median< 80% Saturation. Julian Day designates 3-month DO median aggregating period (e.g. Days 120-210 are May-July and 150-240 are June-August). N= Total number of site events.

Julian Day	Lower South		South		Central		No. Central		San Pablo		Suisun	
	N	**%**	**N**	**%**	**N**	**%**	**N**	**%**	**N**	**%**	**N**	**%**
30-120	**63**	0%	210	0%	82	0%	60	2%	126	1%	96	0%
60-150	**63**	0%	210	0%	82	0%	60	8%	126	4%	96	0%
90-180	**63**	6%	210	0%	82	2%	60	13%	126	3%	96	0%
120-210	**61**	18%	201	0%	80	5%	59	15%	126	1%	100	1%
150-240	**54**	28%	189	1%	77	0%	58	0%	126	0%	97	0%
180-270	**53**	13%	176	0%	73	0%	60	0%	126	0%	94	0%
210-300	**50**	6%	166	0%	68	0%	55	0%	117	0%	89	0%

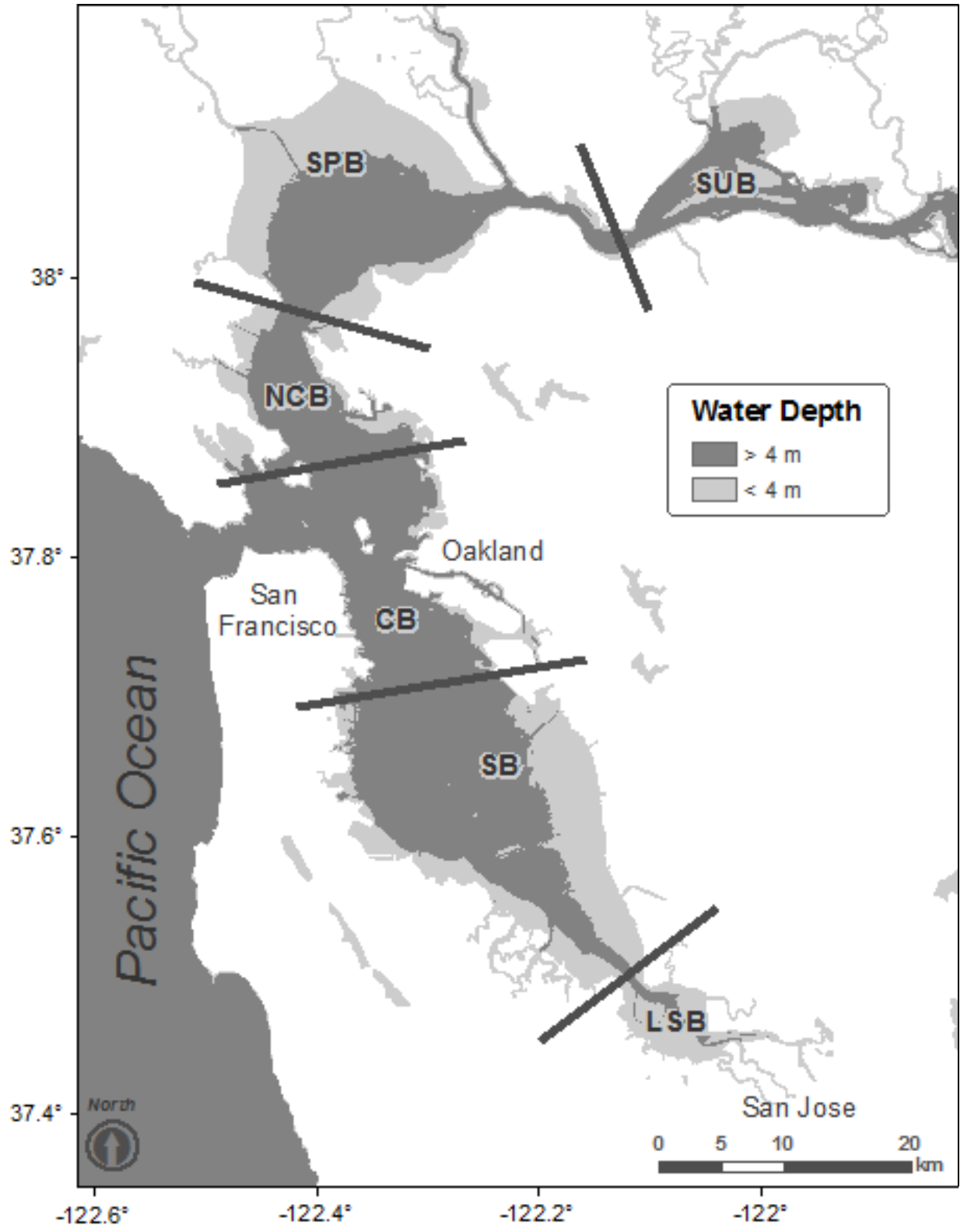
SPB
SUB
NCB
CB
SB
LSB
Water Depth
> 4 m
< 4 m
Oakland
San
Francisco
Pacific Ocean
San Jose
North
0 5 10 20
km
38°
37.8°
37.6°
37.4°
-122.6°
-122.4°
-122.2°
-122°

Fig. 1

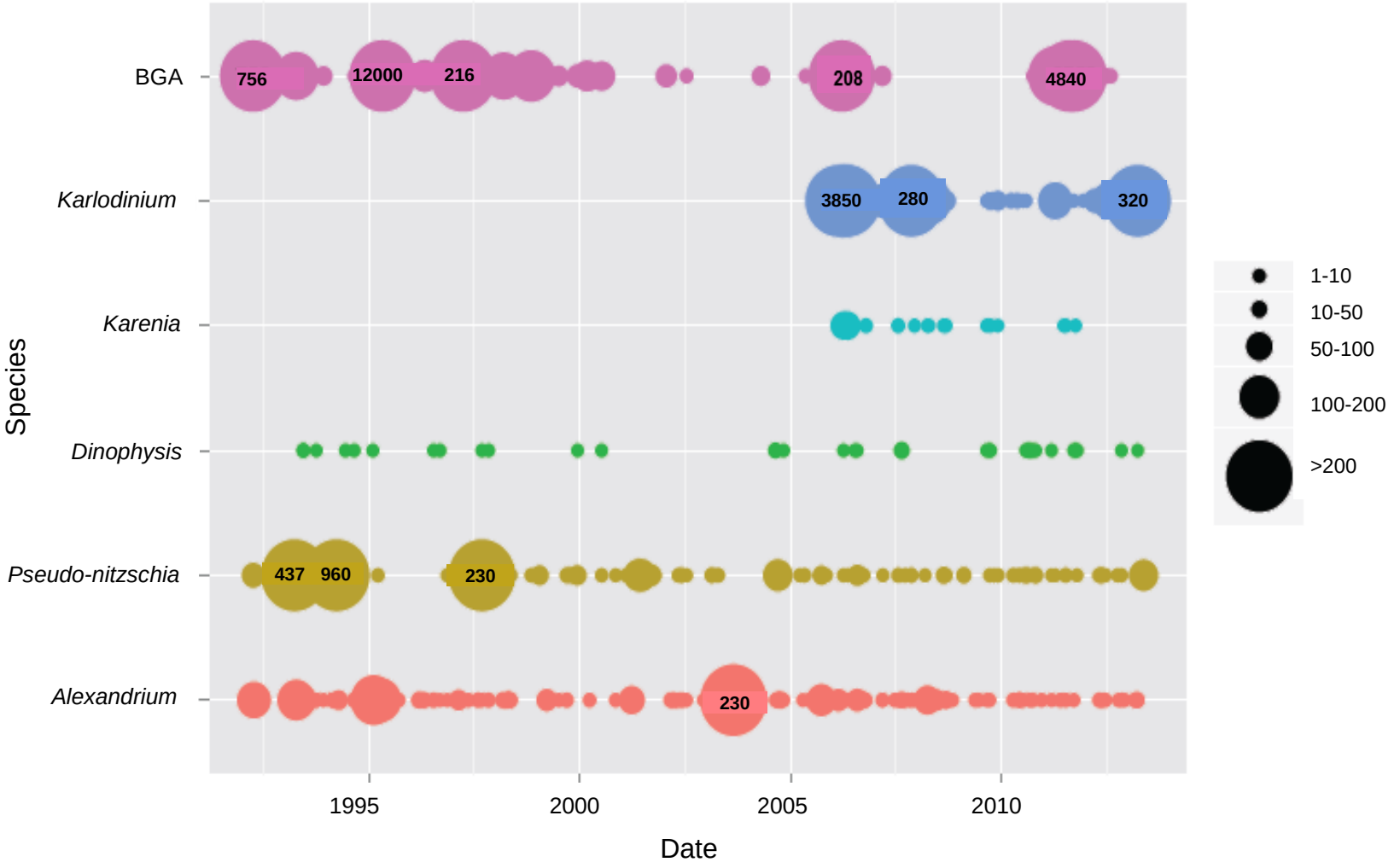
BGA
Karlodinium
Karenia
Dinophysis
Pseudo-nitzschia
Alexandrium
Species
756
12000
216
208
4840
3850
280
320
437
960
230
230
1995
2000
2005
2010
Date
1-10
10-50
50-100
100-200
>200

Fig. 2

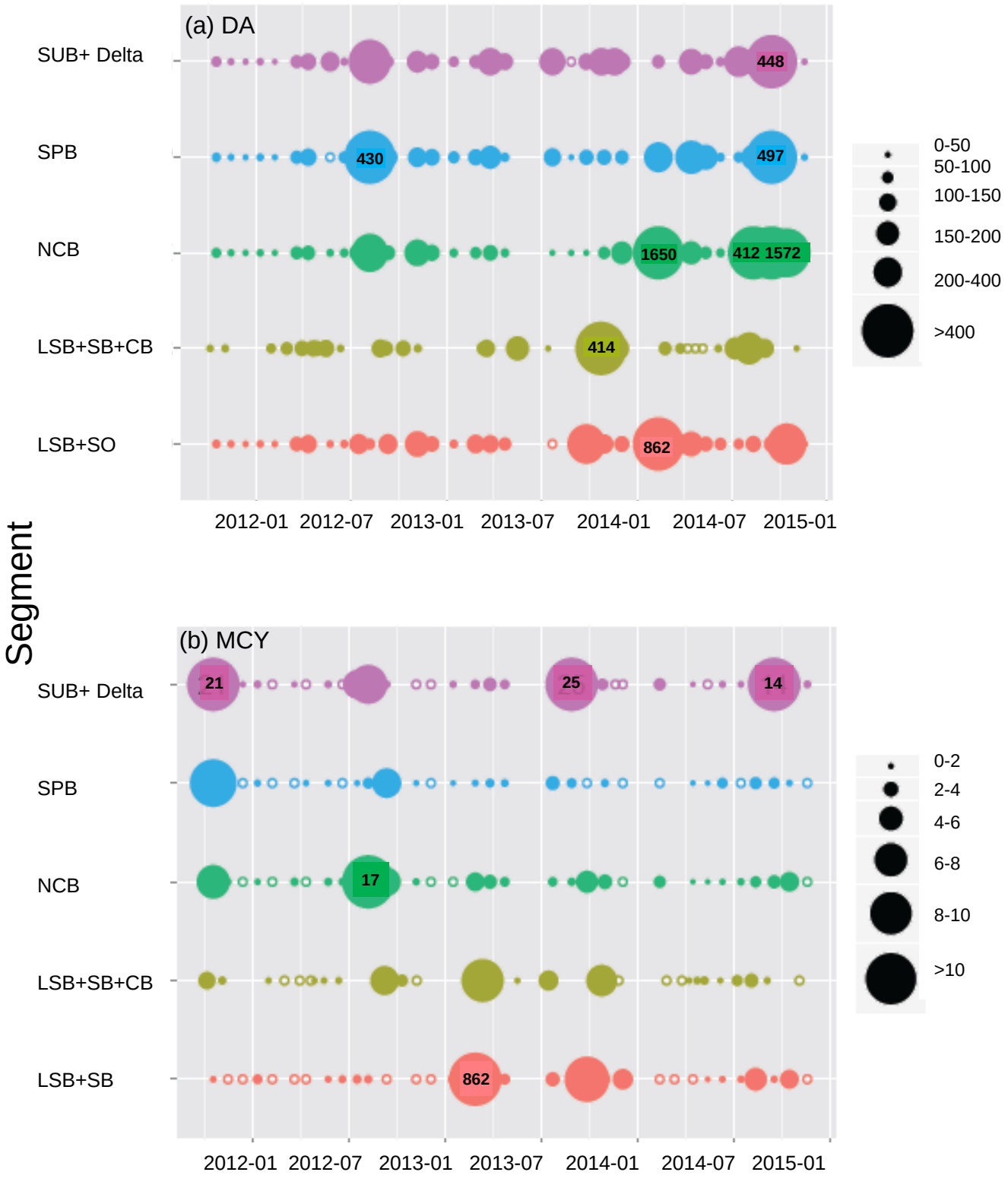
(a) DA
SUB+ Delta
SPB
NCB
LSB+SB+CB
LSB+SO
448
430
497
1650
412 1572
414
862
2012-01
2012-07
2013-01
2013-07
2014-01
2014-07
2015-01
0-50
50-100
100-150
150-200
200-400
>400
(b) MCY
SUB+ Delta
SPB
NCB
LSB+SB+CB
LSB+SB
21
25
14
17
862
2012-01
2012-07
2013-01
2013-07
2014-01
2014-07
2015-01
0-2
2-4
4-6
6-8
8-10
>10
Segment
Date

Fig. 3

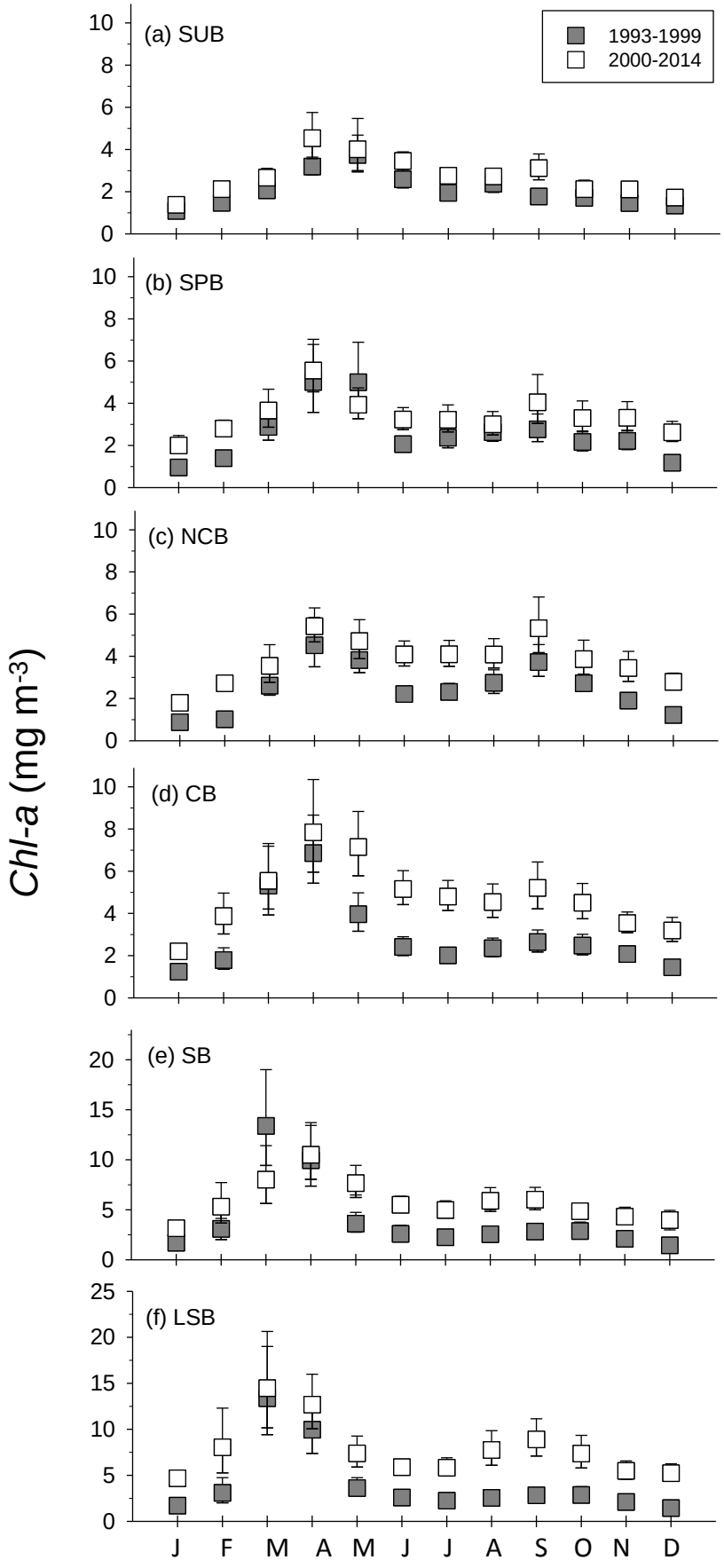
(a) SUB
1993-1999
2000-2014
(b) SPB
(c) NCB
(d) CB
(e) SB
(f) LSB
Chl-a (mg m-3)
J F M A M J J A S O N D
Month

Fig. 4

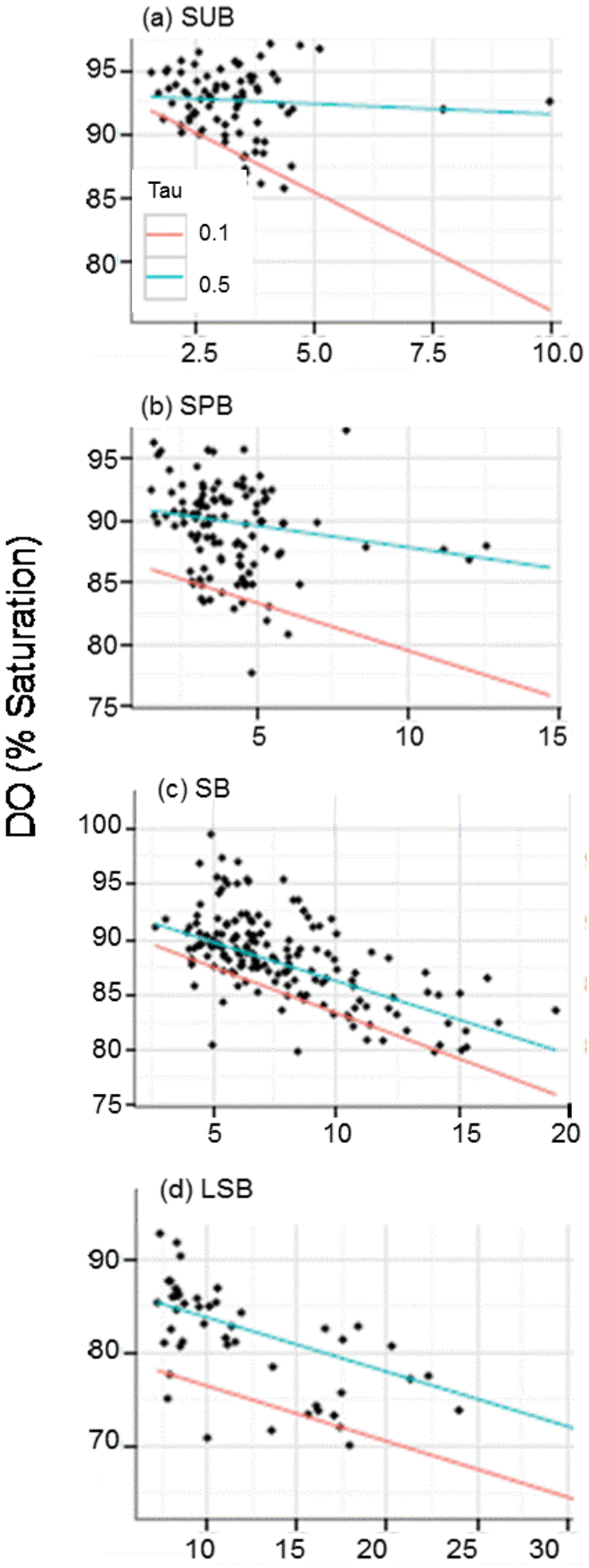
(a) SUB
95
90
85
80
Tau
0.1
0.5
2.5
5.0
7.5
10.0
(b) SPB
95
90
85
80
75
5
10
15
DO (% Saturation)
(c) SB
100
95
90
85
80
75
5
10
15
20
(d) LSB
90
80
70
10
15
20
25
30
Chl-a (mg m-3)

Fig. 5

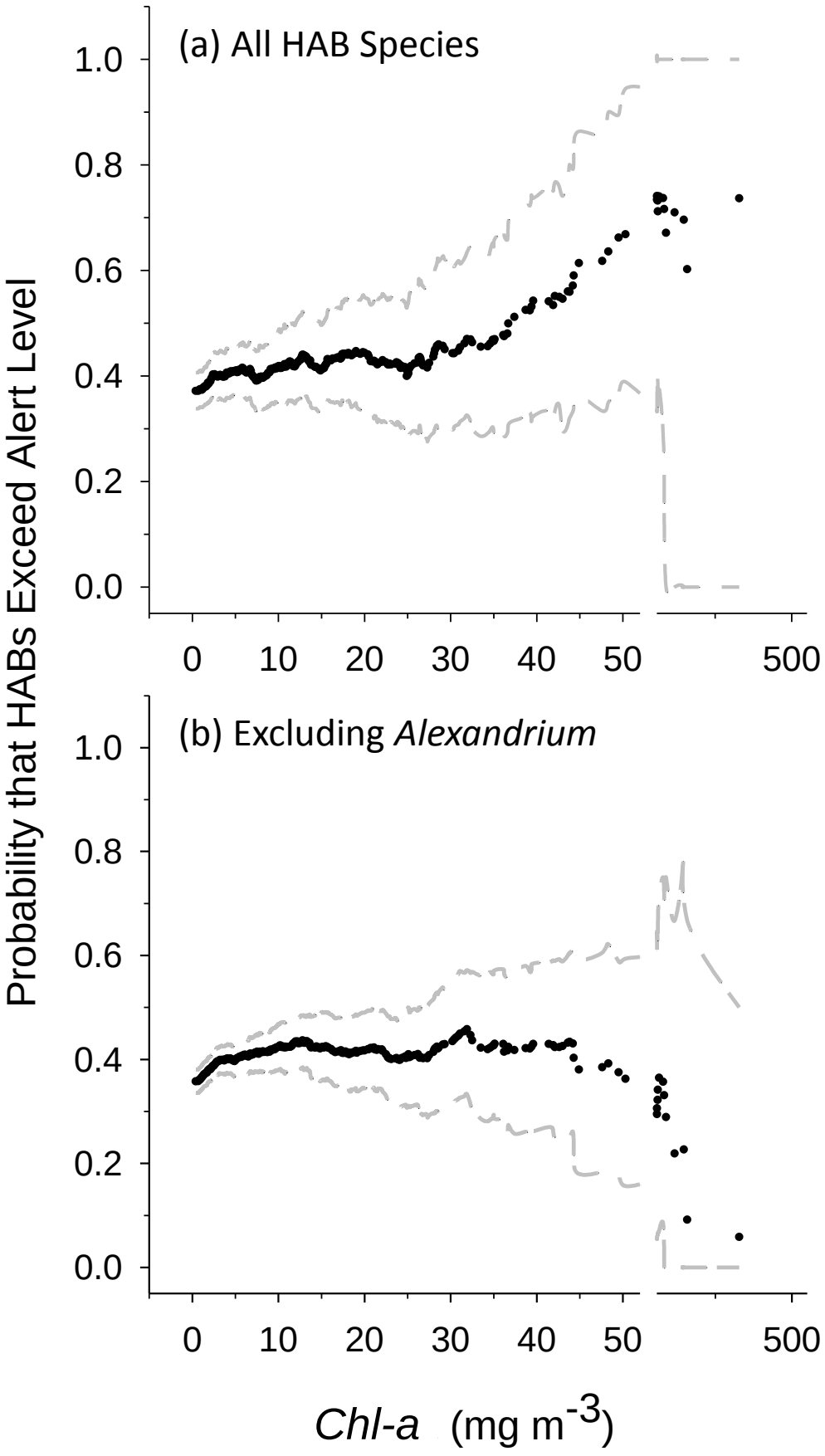
(a) All HAB Species
(b) Excluding *Alexandrium*
Probability that HABs Exceed Alert Level
1.0
0.8
0.6
0.4
0.2
0.0
0
10
20
30
40
50
500
Chl-a (mg m^{-3})

Fig. 6

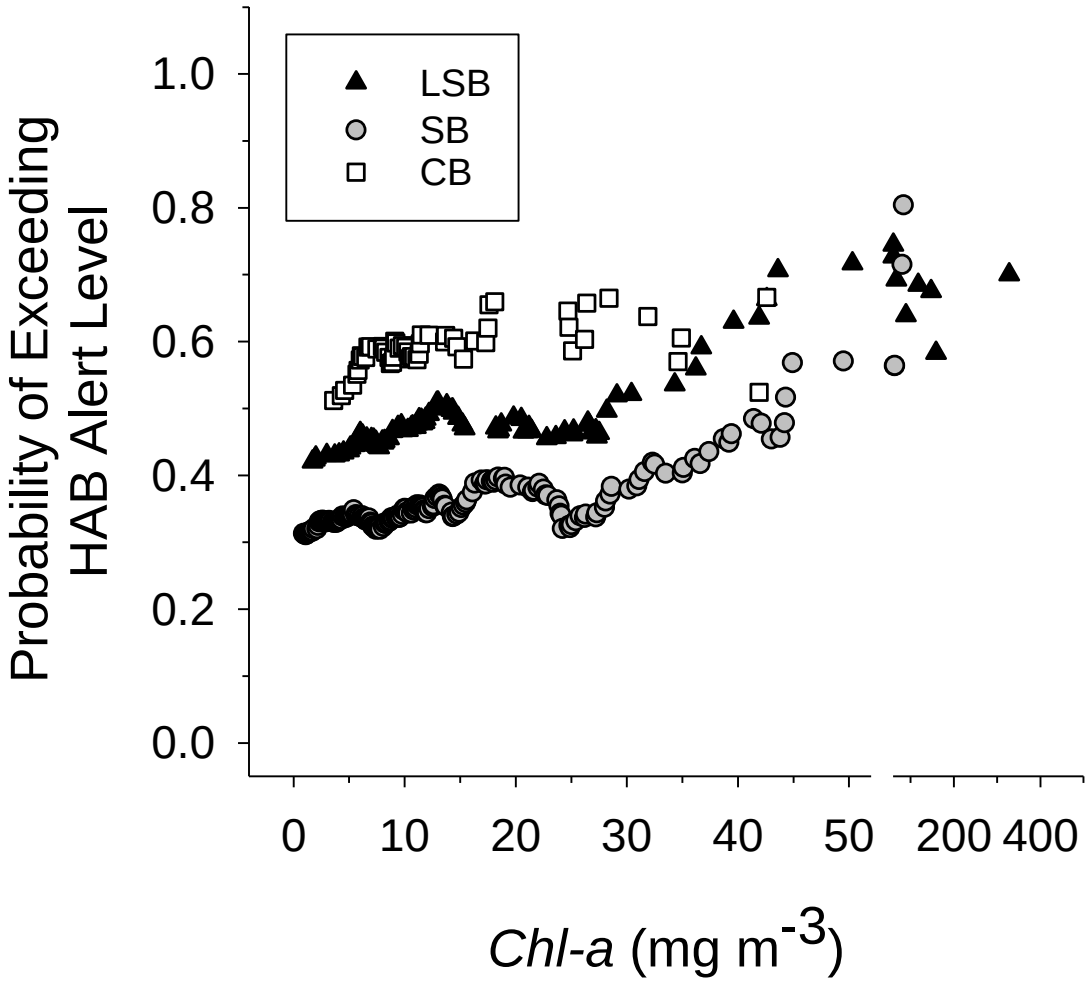
Probability of Exceeding
HAB Alert Level
1.0
0.8
0.6
0.4
0.2
0.0
LSB
SB
CB
0
10
20
30
40
50
200
400
Chl-a (mg m-3)

Fig. 7

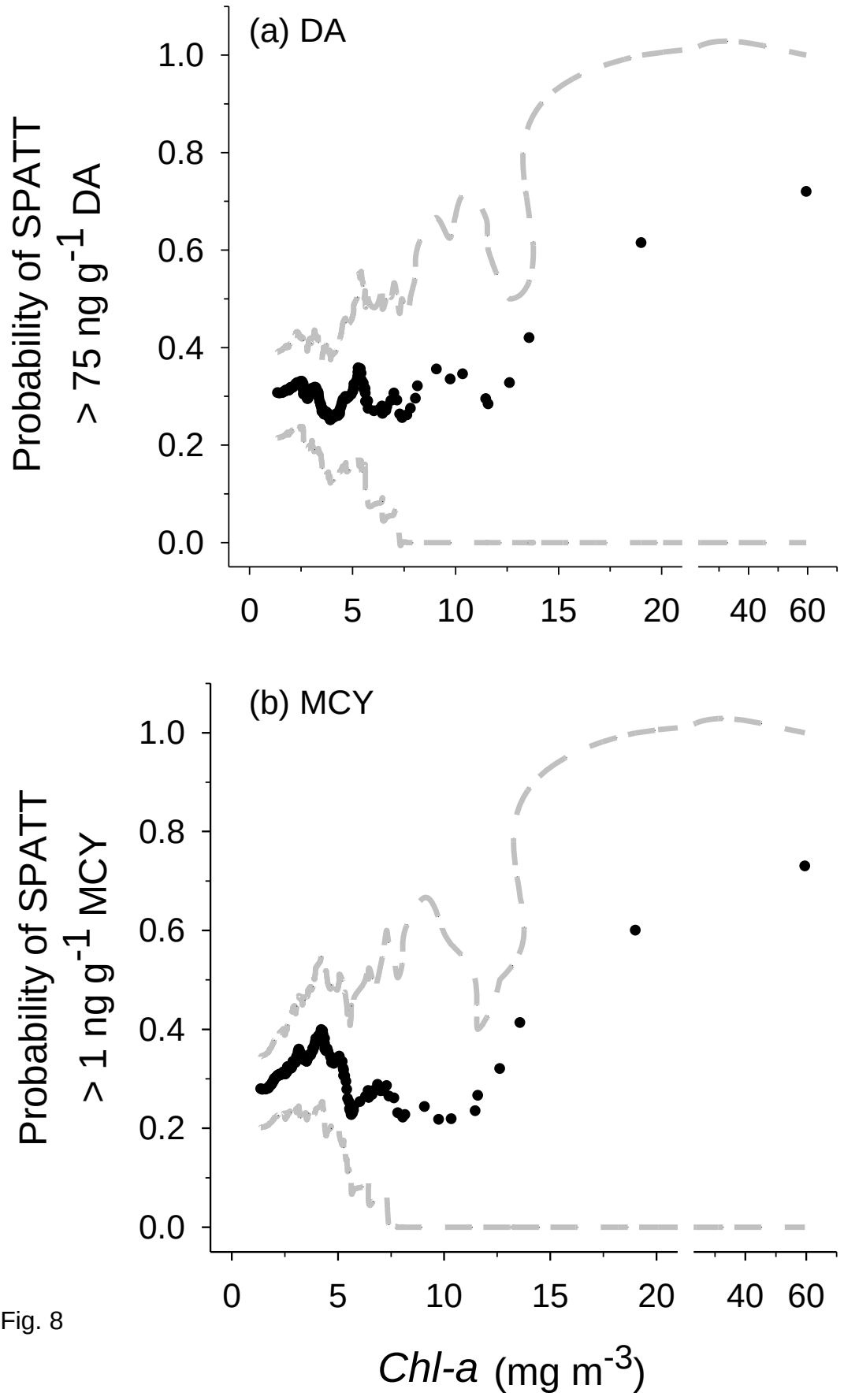
(a) DA
Probability of SPATT
> 75 ng g-1 DA
1.0
0.8
0.6
0.4
0.2
0.0
0
5
10
15
20
40
60
(b) MCY
Probability of SPATT
> 1 ng g-1 MCY
1.0
0.8
0.6
0.4
0.2
0.0
0
5
10
15
20
40
60
Chl-a (mg m-3)

Fig. 8

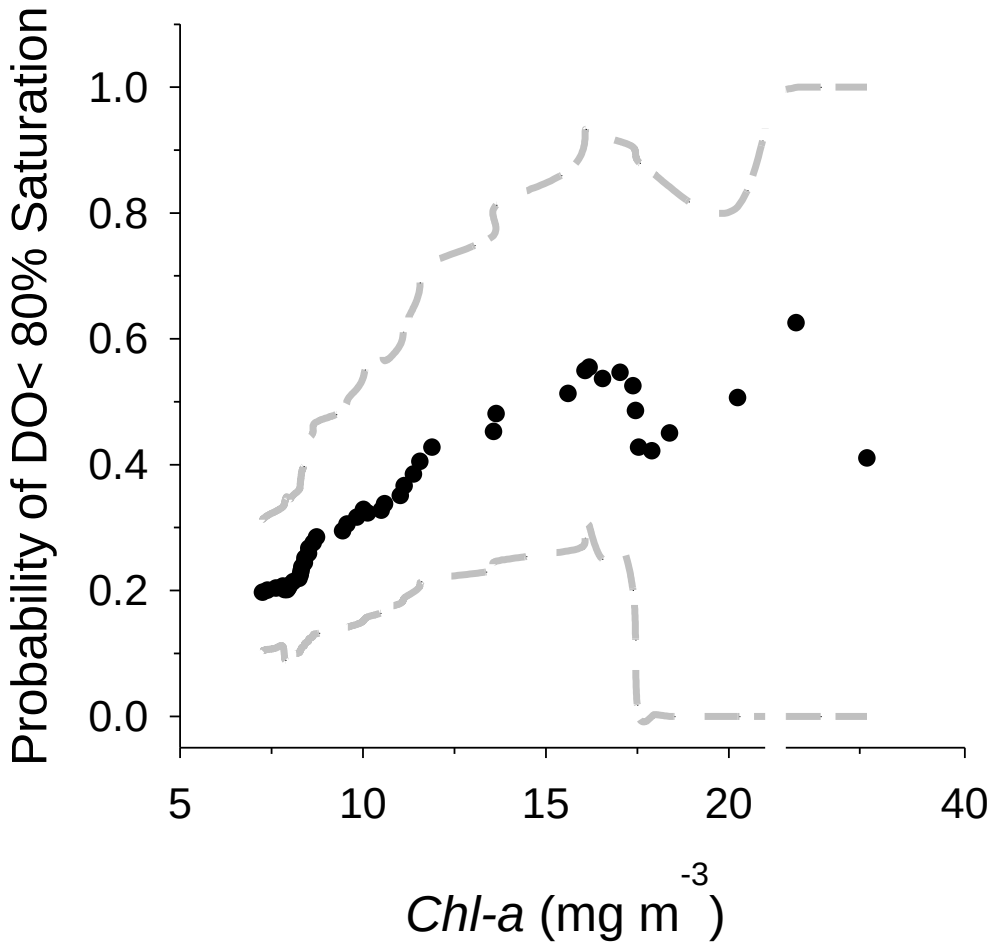
Probability of DO< 80% Saturation
1.0
0.8
0.6
0.4
0.2
0.0
5
10
15
20
40
Chl-a (mg m-3)

Fig 9